Selection of magnetic materials for an active magnetic regenerative refrigerator

C.E. Reid, J.A. Barclay, J.L. Hall and S. Sarangi

Cryofuel Systems Group, University of Victoria, Victoria, B.C. V8W 2Y2 (Canada)

Abstract

High efficiencies of active magnetic regenerative refrigerators (AMRR) are strongly dependent on the correct selection of the magnetic regenerator working material. The selection process involves the thermodynamic analysis of the AMRR cycle to determine the adiabatic temperature change profile (ΔT versus T) over the temperature span of interest for an ideal material, and then the matching of real materials whose magnetocaloric effect (MCE) as a function of absolute temperature best fits this profile. This paper develops the calculation of the ideal magnetic material ΔT versus T profile for a real AMRR operating between 110 and 300 K and with 1 kW of cooling power. The ideal profile was a function of the constant entropy flux from the cold end heat load, the irreversible regenerator entropy production, and other real effects. To accommodate the large temperature span, several magnetic materials were chosen and layered in the regenerator from the cold to the hot end by increasing the Curie temperature. The resultant ΔT versus T curve of the combined material provided only a rough approximation of the calculated ideal material curve. To improve this approximation, physical mixing of magnetic refrigerants was investigated. This procedure diluted the magnetic moment, thereby reducing magnetic entropy available for the cycle. Further, under adiabatic conditions, mixing produced an intolerable amount of entropy during cycle execution. Simple segmentation of the regenerator with more magnetic materials that better match the ideal profile is an easier way to approximate the ideal ΔT versus T curve with real materials. Optimum segmentation will be determined by regenerator complexity.

1. Introduction

Magnetic refrigerators are based on the magnetocaloric effect (MCE) of ferromagnetic materials to achieve cooling. During a simple magnetic refrigeration cycle, magnetized material is periodically put in contact with a high temperature sink and demagnetized material is put in contact with a low temperature source. These steps are linked by adiabatic magnetization and demagnetization processes. This cycle description is generic and could be based on several thermodynamic cycles (Carnot, Brayton, Stirling, etc.). Many rare earth elements have large magnetic entropy changes and therefore may exhibit large MCEs at or near their Curie or ordering temperatures. This feature makes them excellent candidates for the working materials in magnetic refrigerators. The development of ferromagnetic materials for magnetic refrigeration is the focus of several research efforts [1–5].

The temperature span of the above simple magnetic refrigeration cycle is constrained by the magnitude of the magnetocaloric effect of the material used. To extend this temperature span, the addition of a regenerative heat exchanger and a circulating heat transport medium is necessary. The design under investigation in this paper is an active magnetic regenerative refrigerator (AMRR) that spans the temperature range 110–300 K. In this arrangement, the regeneration is accomplished by using several suitable ferromagnetic materials that function as both the thermal storage (passive · regeneration) and as the working material (active regeneration) in the refrigeration cycle. Each infinitesimal element of magnetic material in the AMRR undergoes a unique magnetic cycle as the regenerative magnetic material is cycled in and out of the magnetic field. These elements are linked by the convective heat transport fluid. During the magnetization half of the cycle, the material deposits heat into the fluid where it is subsequently rejected to the environment at the hot end heat exchanger. When the magnetic regenerator cycles out of the field, the fluid deposits heat into the material and can, in turn, pick up the refrigeration load at the cold end heat exchanger. The adiabatic temperature change of each material element is important in the execution of the AMRR cycle. Figure 1 shows the fluid and material temperature profiles for an AMRR during the several stages of the cycle [6].
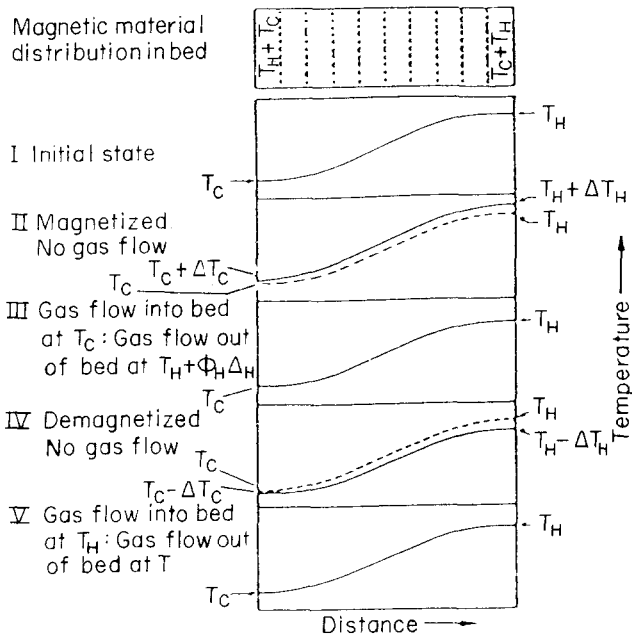
Fig. 1. Temperature profiles during various steps in the operation of an AMRR. Broken lines in frames II and IV indicate the initial state. Fluid enters and exits the regenerator at average temperatures $T_H + \Phi_H \Delta T_H$ and $T_C - \Phi_C \Delta T_C$, where $0 < \Phi_{C,H} < 1$ (taken from ref. 6).

The correct selection and arrangement of the materials used in the AMRR is crucial to achieving high efficiencies in the cycle [1,2,5]. Before real materials are chosen, it is necessary to perform an analysis of the thermodynamic requirements of the AMRR cycle to determine the adiabatic temperature change profile (ΔT versus T curve) for an ideal material. Once this profile is calculated, real materials can be selected and arranged in the regenerator to best fit this ideal curve.

2. Thermodynamic requirements

In an AMRR cycle, the heat transfer fluid picks up an entropy load at the cold end and needs to reject that entropy to the environment. To accomplish this, the magnetic refrigerant needs to provide both active and passive regeneration. The passive regeneration allows the heat transfer fluid to span the temperature gap while the active magnetization and demagnetization of the refrigerant causes a temperature change (ΔT) that allows cooling loads to be accepted at the cold end and subsequently rejected at the hot end. For active regeneration, the critical property of the refrigerant is its adiabatic temperature change as a function of absolute temperature (ΔT versus T) or the MCE. The optimum ΔT versus T curve for a given refrigerant is a function of regenerator position or absolute temperature, the constant entropy flow from the cold source, and any irreversible entropy production in the cycle.

2.1. Ideal (reversible) case

Consider reversible conditions in a AMR refrigeration cycle (i.e. no entropy production, only reversible entropy flow). A direct implication of reversible conditions is that there exists an infinite heat transfer rate between the magnetic solid and the heat transfer fluid in the regenerator. If we further assume that the heat capacity of the circulating heat transport fluid is relatively constant over the temperature range and the material has an infinite thermal mass, the adiabatic temperature change of the material at the cold and hot ends must be directly proportional to the absolute cold and hot end temperatures to conserve entropy flows required by the second law:

$$\dot{Q}_h / \dot{Q}_c = T_h(\Delta s)/[T_c(\Delta s)] = \dot{m}c_p(\Delta T_h)_{\text{fluid}}/[\dot{m}c_p(\Delta T_c)_{\text{fluid}}]$$
$$(1)$$

where $\dot{Q}_h$ is the heat rejected from the fluid at the hot end and $\dot{Q}_c$ is the heat absorbed from the cold space by the fluid at the cold end. With the conservation of the mass of the convective fluid in the cycle, eqn. (1) becomes

$$T_b/T_c = [\Delta T_b/\Delta T_c]_{\text{fluid}}$$
$$(2)$$

and with infinite heat transfer between fluid and solid

$$T_b/T_c = [\Delta T_h/\Delta T_c]_{\text{fluid}} = [\Delta t_h/\Delta T_c]_{\text{solid}}$$
$$(3)$$

Because infinite heat transfer and thermal mass were assumed, the heat transport fluid temperature will track the solid's cycle temperatures exactly with no material thermal energy depletion and the heat energy from the cold source will be pumped and rejected at the hot end heat exchanger with the minimum amount of required work. With the temperature range specified, the above equation effectively sets the magnitude of the adiabatic temperature change required at the hot and cold ends of the regenerator. This argument also sets the optimum ΔT versus T profile of the material across the entire temperature range. In the reversible case, the entropy load from the cold source is to be transported from the cold to the hot end and with no entropy production. This results in a constant entropy flux, and, hence, the adiabatic temperature change must be proportional to the absolute temperature not only at the ends of the regenerator, but also at all temperature positions within the regenerator.

Once the cooling load of the refrigerator has been specified, the ΔT at the cold end of the AMRR can be calculated from the mass flow rate of the circulating fluid:

$$\dot{Q}_c = \dot{m}c_p(\Delta T)_c$$
$$(4)$$

where $(\Delta T)_c$ is the temperature change of the fluid across the load and, in the reversible case, also the
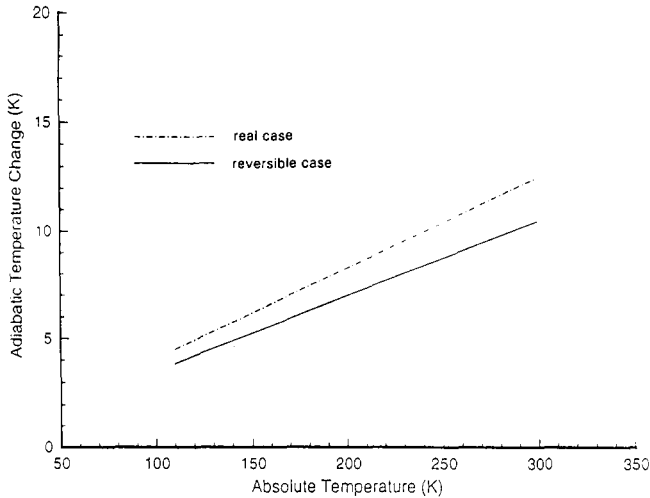
Fig. 2. Calculated adiabatic temperature change as a function of absolute temperature for the ideal material curve for a reversible and real AMRR.

Fig. 3. Reciprocating active magnetic regenerative concept (taken from ref. 7).

adiabatic temperature change of the material (or the MCE). With $(\Delta T)_c$ established, the value of $(\Delta T)_h$ can be calculated from eqn. (3). To operate this cycle reversibly, the regenerator must be made from materials that exhibit a $(\Delta_T)_c$ at 110 K and increase linearly to almost three times this value at 300 K.

Figure 2 shows the adiabatic temperature change profile of the ideal material on a ΔT versus T graph for a reversible AMRR with 1 kW of cooling power operating with 2.0 MPa helium circulating at 0.1 kg s^{-1}. The results show a required $(\Delta T)_c$ of 3.85 K and a $(\Delta T)_h$ of 10.5 K. In the figure, the adiabatic temperature change increases linearly with the absolute temperature according to eqn. (5). The refrigerator has a reciprocating regenerator that cycles at 1 Hz through an 8 T magnetic field and is configured as in Fig. 3 [7].

2.2. Entropy production and real effects

A real magnetic cycle based on the AMRR will not be reversible but will generate a finite amount of entropy during operation. The adiabatic temperature change profile for the ideal material in the AMRR changes when entropy generation mechanisms are taken into account. In the reversible case, the required ΔT versus T profile is evaluated by eqn. (3). In the case where irreversibilities are present, these equations are no longer complete. If we consider only the regenerative component of the refrigerator cycle, the total entropy generation rate (S) can be expressed as the sum of three mechanisms [6]:

$$\dot{S}_{bt} = [\dot{Q}_r/(N_{tu} + 1)](1/T_c - 1/T_h) \tag{5}$$

where $\dot{S}_{ht}$ is the entropy generation rate due to finite heat transfer between solid and fluid and $\dot{Q}_r$ is the heat transfer rate of the regenerator and N_{tu} is the
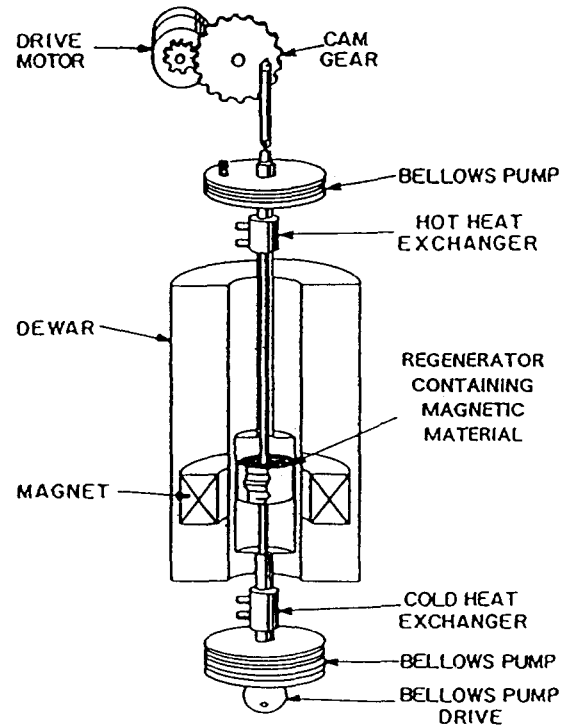
average number of heat transfer units of the regeneration,

$$\dot{S}_{vd} = V_f \, \Delta P/T_h \tag{6}$$

where $\dot{S}_{vd}$ is the entropy generation rate due to viscous dissipation, V_f is the average volume flow rate, and ΔP is the pressure drop across the bed, and finally

$$\dot{S}_{cond} = (\lambda A_c/L)(T_h - T_c)^2/(T_h T_c) \tag{7}$$

where $\dot{S}_{cond}$ is the entropy generation rate due to axial conduction and gas dispersion along the bed, λ is the effective thermal conductivity, L is the regenerator length, and A_c is the cross-sectional area. The total entropy generation rate is

$$\dot{S}_{gen} = \dot{S}_{bt} + \dot{S}_{vd} + \dot{S}_{cond} \tag{8}$$

The effect of the generated entropy will be to increase the actual net work by $T_h \dot{S}_{gen}$:

$$W_{act} = \dot{Q}_c(T_h/T_c - 1) + T_h \dot{S}_{gen} \tag{9}$$

The coefficient of performance of the refrigerator (η) will then be the ratio of reversible work to actual work. With entropy generation, the ΔT versus T contour of the ideal regenerative magnetic refrigerant is more complicated because the fluid temperature changes are no longer the same as those for the material. Only the adiabatic temperature change of the heat transport fluid undergoes proportional scaling in the regenerator and this scaling will be magnified by the regenerator

inefficiency. Equation (3) must be modified to take these, as well as other real effects, into account. We can make this quantitative by assuming that the entropy is generated uniformly throughout the regenerator. Equation (3) becomes

$$\Delta T_h = \Delta T_c + (\Delta T_c - \Delta T_{reg} - \Delta T_w)(T_h - T_c)/T_c/\eta_r \qquad (10)$$

where ΔT_h and ΔT_c are the material adiabatic temperature changes for a real cycle at the regenerator hot and cold ends, ΔT_{reg} is the temperature difference between solid and fluid due to finite heat transfer, ΔT_w is the average thermal washing effect (the temperature change of the material caused by its finite thermal mass compared to that of the convective heat transfer fluid), and η_r is the figure of merit where the real work takes into account only $\dot{S}_{ht}$ and $\dot{S}_{cond}$ (i.e. viscous dissipation effects are manifested as increased compressor work). If ΔT_{reg} and ΔT_w in eqn. (10) are set to zero, eqn. (3) for the reversible case is recovered as expected. The real ΔT_c from eqn. (10) is related to the reversible ΔT_c from (3) by

$$\Delta T_c(\text{real}) = \Delta T_c(\text{reversible}) + \Delta t_{reg} + \Delta T_w \qquad (11)$$

The effect of entropy production in a real cycle will be to change the slope of the required material ΔT versus T curve. Whether the slope will increase or decrease is a function of the combined variables in eqn. (10).

For a real AMRR cycle, operating under conditions outlined above with a regenerator bed composed of 0.25 mm particles, the entropy generated will be: $\dot{S}_{ht} = 0.409$ W K^{-1}, $\dot{S}_{vd} = 2.30$ W K^{-1}, and $\dot{S}_{cond} = 0.797$ W K^{-1}. The figure of merit for the cycle is 0.622 and the $\eta_r = 0.827$. With a ΔT_{reg} of 0.15 K and ΔT_w of 0.5 K, the real ΔT_c is 4.50 K and ΔT_h is 12.5 K (from eqn. (10)). Figure 2 shows the adjusted ΔT versus T curve of the best material for this real AMRR cycle. The linear profile is preserved under the given assumptions because the entropy will be generated uniformly along the length of the regenerator.

3. Material selection

With the required ΔT versus T curve for the ideal working material in the real cycle established by the above analysis, an existing material or materials must be selected whose MCE as a function of temperature and applied field closely approximates this curve.

3.1. Single material

The best case for material selection is to use a single material whose profile closely matches the ideal curve for the real case in Fig. 2. Considering the typical sharp peak shape of a ferromagnetic material's MCE profile,

the single material would have to have an extremely large adiabatic temperature change (at 8 T) with its maximum or Curie point well above 300 K. Other materials that exhibit more complicated magnetic ordering might not have the classical peak shaped. To be useful, these materials must magnetically order so that their ΔT versus T profile closely resembles that of the ideal material. Because such materials have not been discovered, the selection process will invariably involve the choice of several materials that will be carefully layered in the regenerator.

3.2. Layered materials

To successfully span the temperature range of the working design, several carefully chosen materials will need to be stacked in the regenerator from the cold to the hot end. Figure 4 shows the adiabatic temperature change curves for real and hypothetical materials superimposed over the calculated ideal material curve for the real case. The MCE for all materials was calculated using a molecular field simulation program. The MCE results from the model are for ferromagnetic, isotropic materials and have been validated with actual MCEs of magnetic materials that exhibit the assumed properties [8–11]. From the figure, the useful ranges of the existing rare earth materials in the AMRR are approximately 270–300 K for Gd, 220–240 K for Tb and 170–185 K for Dy. The other materials could be rare earth alloys, intermetallic compounds or even magnetic nanocomposites. The actual MCE profile for dysprosium has a bump on the left slope due to the destruction of the helicoidal antiferromagnetic phase at high applied fields. In reality, this bump might help to approximate the ideal curve at the low temperature end and render some of materials C, D, and E redundant. With the
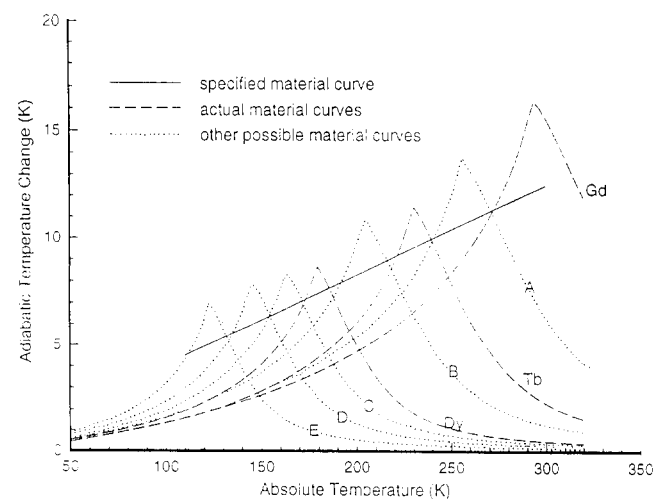

Fig. 4. Adiabatic temperature change as a function of absolute temperature for ideal material curve (real AMRR case), existing rare earths, and hypothetical material curves to span the AMRR temperature range.

above material selection, the working design temperature range has now been completely covered. Figure 5 shows how these materials would actually be stacked in the AMRR. This assumes that the temperature profile in the regenerator will be linear in the axial flow direction and that each material segment behaves independently.

3.3. Improving combined material ΔT versus T curves

Layering real materials in the regenerator will provide only a rough approximation to the ideal material curve (see Fig. 5). Any deviation from the calculated ΔT versus T profile will result in extra entropy generation beyond those already discussed. The magnitude of this irreversibility is hard to ascertain, as is the overall effects of a positive versus a negative deviation. To obtain a better approximation, more materials could be selected, each spanning an increasing smaller temperature range. This procedure will allow the peaks of the combined material curve to fall towards the ideal curve with applied field reduction and is primarily limited by the complexity of oversegmenting in the regenerator.

Another possible way that real materials could be used to achieve a better approximation to the ideal curve is by physical mixing. If materials of different MCE profiles are mixed in the right proportions, the peaks in Fig. 5 could be smoothed out to match the specified curve. With physical mixing , however, there will be finite temperature difference heat transfer between materials with different adiabatic temperature changes and, consequently, entropy generation. The easiest mixing case is to analyse a material that is not magnetic (has no MCE) and to merely add it to the regenerator in varying proportions to dilute the magnetic

materials. Calculations were performed to estimate the entropy production due to mixing materials to reduce the terbium adiabatic temperature change peak in Fig. 5 to the specified curve line. The calculations involved the addition of aluminum particles of the same diameter as the magnetic metal to the terbium section of the regenerator. The mass of the diluting material added is a function of the difference between the T of the specified curve and the T of terbium. The entropy generated was calculated from

$$\dot{\sigma} = (\dot{m}C_p)_{Tb} \ln(T_{req}/T_{Tb}) + (\dot{m}C_p)_{Al} \ln(T_{req}/T_{Al}) \qquad (12)$$

where T_{req} is the absolute temperature of the specified curve, T_{Tb} and T_{Al} are the absolute temperatures of the mixed aluminum and terbium particles immediately after magnetization and the masses are the amounts of both materials in the terbium segment of the regenerator. The mass of terbium was calculated from an energy balance between the helium transport fluid and the regenerator material:

$$(\dot{m}C_p)_{Tb} \, \Delta T_w = (\dot{m}C_p)_{He}\Delta T_{He} \qquad (13)$$

where ΔT_{He} is the change in the fluid's temperature as it flows through the terbium section. The mass of aluminum required to shave the terbium peak was calculated from an energy balance between the aluminum and terbium material in the terbium segment:

$$(\dot{m}c_p)_{Al} \, \Delta T_{req} = (\dot{m}c_p)_{Tb}(\Delta T_{Tb} - \Delta T_{req}) \qquad (14)$$

where ΔT_{req} is the adiabatic temperature change of the specified curve and ΔT_{Tb} is the adiabatic temperature change of the terbium in the section.

The result of adding aluminum to the terbium was an additional entropy generation of 2.7 W K^{-1}. This produces an additional load of 810 W at the hot end of the AMRR. This mixing entropy is already on the same order as all other entropy generation mechanisms combined. To mix materials in this manner through the entire regenerator to achieve the specified curve profile would produce an enormous energy load. It would also change the profile of the ideal material curve calculated from eqn. (11) because the entropy will no longer be just a function of longitudinal conduction and fluid/solid heat transfer nor will it be uniformly generated throughout the regenerator. Physical mixing of materials can only be feasible if a more intimate contact between the different materials is achieved. If the heat transfer rate between substances could be accelerated to the same order as the lattice heat transfer caused by the MCE, the entropy generation due to mixing would be essentially zero. This, however, requires contact on an atomic scale.
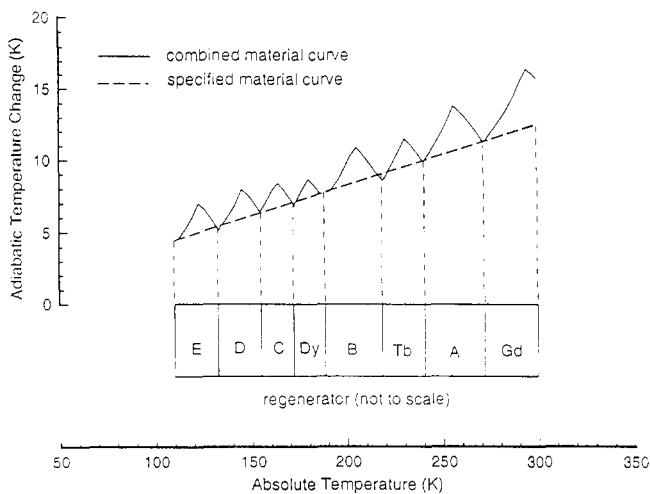

Fig. 5. Adiabatic temperature change as a function of absolute temperature of the combined materials. Figure also shows proposed segmentation of regenerator into material segments.

4. Conclusion

The adiabatic temperature change profile (ΔT versus T curve) for the ideal working material in an AMRR

is a function of the constant entropy flux from the cold end heat load, the cumulative influences of entropy generation in the regenerator itself, and other real effects. If the entropy is generated uniformly from the cold to the hot end, then the ideal material curves are linear. The slope of these ideal curves will be affected by the magnitudes of regenerator entropy generation, the fluid/solid temperature approach and the thermal washing of the material. To approximate the ideal material curve for a simple AMRR with a 190 K temperature span and 1 kW of cooling power, several different magnetic materials were stacked in the regenerator bed. Each material in this stack had an increasing Curie temperature according to position from the cold to hot end. This stacking provided a regenerator whose ΔT versus T curve is a rough approximation to the ideal curve. The match of the ΔT versus T curves between the stacked materials in the regenerator and the ideal material can easily be improved by further segmentation of the regenerator into more magnetic material refrigerant sections that cover the temperature span. Such discretization lowers the peaks in the ΔT versus T curve of the combined materials towards the ΔT versus T curve of the ideal material but increases the complexity of the design. Mixing of materials to flatten the peaks of the ΔT versus T curve of the stacked materials in the regenerator is counterproductive because this process dilutes the material's magnetic moment and generates entropy. It is doubtful that cycle inefficiencies caused by deviations from the ideal material curve (due to the rough approximation of the stacked materials in the regenerator) will outweigh the inefficiency caused by the large heat load generated by simple macroscopic material mixing. However, further

analysis is required to determine the thermodynamic cost of any deviation from the ideal material curve. This will be necessary to ascertain the number of magnetic refrigerants and the subsequent regenerator segmentation required to achieve optimum approximation to the ideal magnetic refrigerant adiabatic temperature change curve.

Acknowledgements

References

1 C.R. Cross *et al.*, Optimal temperature-entropy curves for magnetic refrigeration, Astronautics Technology Center, Madison, WI.
2 J.L. Smith, Jr., Y. Iwasa and F.J. Cogswell, *Adv. Cryog. Eng.*, *35* (1990) 1157.
3 T. Hashimoto *et al.*, *Cryogenics, Nov.* (1981) 647.
4 C.B. Zimm *et al.*, *Adv. Cryog. Eng.*, *37B* (1992) 883.
5 S.R. Schuricht, A.J. Gregoria and C.B. Zimm, The effects of a layered bed on active magnetic regenerator performance, *Int. Cryocooler Conf.*, 1992.
6 J.A. Barclay and S. Sarangi, Selection of regenerator geometry for magnetic refrigeration, *Cryog. Processes Equip.*, 1984.
7 J.A. Barclay, An analysis of liquefaction of helium using magnetic refrigerators, Los Alamos National Laboratory Report, 1981, LA-8991.
8 A.S. Andreenko *et al.*, *Ups. Fiz. Nauk*, *158* (1989) 553.
9 S.A. Nikitin, A.M. Tishin and P.I. Leontev, *Phys. Status Solidi (a)*, *113* (1989) K117.
10 C.B. Zimm, P.L. Kral and J.A. Barclay, The magnetocaloric effect in erbium, *Proc. 5th Int. Cryocooler Conf.*, 1988.
11 S.A. Nikitin *et al.*, *Phys. Met. Metall.*, *59* (1985) 104.